

# Creation and annihilation of phase singularities near a sub-wavelength slit

Hugo F. Schouten<sup>1</sup>, Taco D. Visser<sup>1\*</sup>, Greg Gbur<sup>1</sup>,  
Daan Lenstra<sup>1</sup>, and Hans Blok<sup>2</sup>

<sup>1</sup>*Department of Physics and Astronomy  
Free University, Amsterdam, The Netherlands*

<sup>2</sup>*Department of Electrical Engineering  
Delft University of Technology, Delft, The Netherlands*

[\\*twisser@nat.vu.nl](mailto:twisser@nat.vu.nl)

**Abstract:** The anomalously-high transmission of light through sub-wavelength apertures is a phenomenon which has been observed in numerous experiments, but whose theoretical explanation is incomplete. In this article we present a numerical analysis of the power flow (characterized by the Poynting vector) of the electromagnetic field near a sub-wavelength sized slit in a thin metal plate, and demonstrate that the enhanced transmission is accompanied by the annihilation of phase singularities in the power flow near the slit.

© 2003 Optical Society of America

**OCIS codes:** (260.2910) Electromagnetic theory, (050.1220) Apertures, (050.1960) Diffraction theory, (999.9999) Singular Optics

---

## References and links

1. J.F. Nye and M.V. Berry, "Dislocations in wave trains," *Proc. Roy. Soc. Lond. A* **336**, 165-190 (1974).
2. J.F. Nye, *Natural Focusing and the Fine Structure of Light* (Institute of Physics, Bristol, 1999).
3. M.S. Soskin and M.V. Vasnetsov, "Singular Optics", in *Progress in Optics* **42**, ed. E. Wolf (Elsevier, Amsterdam, 2001), 219-276.
4. T.W. Ebbesen, H.J. Lezec, H.F. Ghaemi, T. Thio and P.A. Wolff, "Extraordinary optical transmission through sub-wavelength hole arrays," *Nature* **391**, 667-669 (1998).
5. T. Thio, K.M. Pellerin, R.A. Linke, H.J. Lezec and T.W. Ebbesen, "Enhanced light transmission through a single subwavelength aperture," *Opt. Lett.* **26**, 1972-1974 (2001).
6. A. Boivin, J. Dow and E. Wolf, "Energy flow in the neighborhood of the focus of a coherent beam," *J. Opt. Soc. Am.* **57**, 1171-1175 (1967).
7. F. Landstorfer, H. Meinke and G. Niedermair, "Ringförmiger Energiewirbel im Nahfeld einer Richtantenne," *Nachrichtentechn. Z.* **25**, 537-576 (1972).
8. G.P. Karman, M.W. Beijersbergen, A. van Duijl, and J.P. Woerdman, "Creation and annihilation of phase singularities in a focal field," *Opt. Lett.* **22**, 1503-1505 (1997).
9. T.D. Visser, H. Blok and D. Lenstra, "Theory of polarization-dependent amplification in a slab waveguide with anisotropic gain and losses," *IEEE J. Quant. Elect.* **35**, 240-249 (1999).
10. H.F. Schouten, T.D. Visser, D. Lenstra and H. Blok, "Light transmission through a sub-wavelength slit: waveguiding and optical vortices," *Phys. Rev. E*, in press.
11. D.E. Gray, ed., *American Institute of Physics Handbook* (McGraw-Hill, New York, 1972, 3rd edition).

---

## 1. Introduction

It has been known now for some time that the phase of a wavefield can exhibit unusual behavior in the neighborhood of points where the amplitude of the field is zero. This unusual behavior is connected to the fact that the phase of the field is undefined when

the amplitude vanishes. The systematic study of such singular points, initiated by Nye and Berry [1], has developed into a vibrant field of optics, now usually called singular optics [2, 3]. The phase of the field in the neighborhood of such singular points can exhibit a rich variety of behaviors, such as vortices and dislocations. Furthermore, it is well-known that these singular points possess certain conserved quantities, such as topological charge, and may only be created and annihilated in ways which satisfy certain conservation laws.

A seemingly unrelated field of research that has been investigated in recent years is the study of anomalous light transmission through sub-wavelength sized apertures in thin plates. Ebbesen *et al.* demonstrated experimentally [4] that certain arrays of cylindrical cavities in metal plates allow much more light transmission than predicted by the standard theory of aperture diffraction. These authors suggested that this enhanced transmission was generated by the coupling of the light to surface plasmons in the metal. More recently, it was demonstrated [5] that enhanced transmission can be achieved even with the use of a single aperture. A good understanding of the causes and requirements for such enhanced transmission could lead to, among other things, novel near-field optical measurement devices as well as optical storage devices with a density not restricted by the diffraction limit.

In this article we describe two-dimensional numerical simulations we have undertaken of the electromagnetic field in the neighborhood of a sub-wavelength sized slit in a thin metal plate. In particular, the behavior of the time-averaged Poynting vector is analyzed using a rigorous integral equation method. It is found that the field of power flow in the vicinity of the slit typically possesses numerous phase singularities. More importantly, it is found that the annihilation of phase singularities coincides with the onset of extraordinary light transmission through the slit. Furthermore, the incident field is taken to be TE polarized, which does not allow for the excitation of surface plasmons; this demonstrates that enhanced transmission can occur even in their absence. Our analysis suggests that a good understanding of enhanced transmission requires that the behavior of the phase singularities of the field be taken into account.

## 2. Singular optics of electromagnetic fields

In our analysis, we are interested in the singular optics of a real-valued vector field, namely the two-dimensional time-averaged Poynting vector field,

$$\mathbf{S}(x, z) = \frac{1}{2} \text{Re} \left\{ \hat{\mathbf{E}}(x, z) \times \hat{\mathbf{H}}^*(x, z) \right\}, \quad (1)$$

where  $\hat{\mathbf{E}}$  and  $\hat{\mathbf{H}}$  are the amplitudes of a complex monochromatic electromagnetic field (of time dependence  $\exp[-i\omega t]$ ).

The phase  $\phi_S$  of the Poynting vector is given by the pair of relations

$$\begin{aligned} \sin \phi_S(x, z) &\equiv \frac{S_z(x, z)}{|\mathbf{S}|}, \\ \cos \phi_S(x, z) &\equiv \frac{S_x(x, z)}{|\mathbf{S}|}, \end{aligned} \quad (2)$$

where  $|\mathbf{S}|$  is the modulus of  $\mathbf{S}$ . It follows from these equations that  $\phi_S(x, z)$  is singular whenever  $\mathbf{S} = 0$ . Electromagnetic systems which exhibit singularities of power flow have been known of for some time [6, 7], and the creation and annihilation of singularities in such systems has been studied [8].

For a field which is TE polarized, i.e. the only component of the electric field is  $\hat{E}_y$ ,

it can be readily shown using Eq. (1) and Maxwell's equations that

$$\mathbf{S}(x, z) = -\frac{1}{2\omega\mu_0} \text{Im} \left\{ \hat{E}_y \nabla \hat{E}_y^* \right\}. \quad (3)$$

We may express  $\hat{E}_y$  as an amplitude and phase,

$$\hat{E}_y(x, z) = |\hat{E}_y(x, z)| e^{i\phi_E(x, z)}. \quad (4)$$

On substituting from Eq. (4) into Eq. (3), one immediately finds that the Poynting vector may be expressed in the form

$$\mathbf{S}(x, z) = \frac{1}{2\omega\mu_0} |\hat{E}_y(x, z)|^2 \nabla \phi_E(x, z). \quad (5)$$

This equation suggests that the singular points of  $\mathbf{S}$  may generally be divided into two categories: those which are related to the singular points of the phase of  $\hat{E}_y$  (when  $|\hat{E}_y(x, z)| = 0$ ) and those which are related to the stationary points of the phase of  $\hat{E}_y$  (for which  $\nabla \phi_E(x, z) = 0$ ). Because these topological features of  $\hat{E}_y$  are directly related to the singular points of  $\mathbf{S}$ , we will briefly review some properties of the singular and stationary points of  $\hat{E}_y$  and their relation to the singular points of  $\mathbf{S}$ .

The phase around a singular point of a complex scalar field is well-known to possess a vortex-like structure (as described for instance in [3]). The phase increases or decreases as one moves about the singular point in a counterclockwise direction; the vortex is then referred to as positive or negative, respectively (see Fig. 1(a)). The phase vortices of  $\hat{E}_y$  correspond to vortices (also referred to as centers) of the power flow  $\mathbf{S}$ , around which the power flow circulates (see Fig. 1(b)). A center is referred to as right-handed (left-handed) if it is counterclockwise with respect to the positive (negative)  $y$ -axis. It is to be noted that in all the figures in this article the  $y$ -axis points into the page; a left-handed or right-handed center therefore corresponds to a positive or negative phase vortex, respectively.

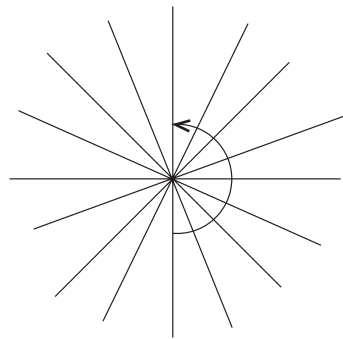
At stationary points of a complex scalar field, the phase is well-defined but its gradient vanishes. Stationary points includes both minima and maxima as well as saddles, to be referred to as phase saddles (Fig. 1(c)). Phase saddles of  $\hat{E}_y$  correspond to saddle points of the power flow, as illustrated in Fig. 1(d). A phase maximum (Fig. 1(e)) of  $\hat{E}_y$  corresponds to a sink of power flow (Fig. 1(f)), and a phase minimum corresponds to a source of power flow; it is to be noted that sinks and sources do not occur in free space.

Both phase singularities and stationary points are topological features of the complex field  $\hat{E}_y$ , and several conserved quantities can be associated with each topological feature. The first of these is the so-called *topological charge*  $s_E$  of the field, defined as the integral of  $\nabla \phi_E$  around a closed loop enclosing the feature such that

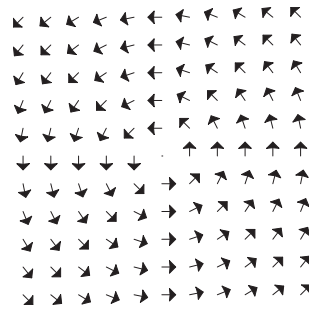
$$s_E \equiv \frac{1}{2\pi} \oint_C \nabla \phi_E \cdot d\mathbf{r}, \quad (6)$$

where  $C$  is a closed counterclockwise path of winding number 1. It can be shown that the topological charge of a given phase singularity takes on a unique positive or negative integer value, independent of the choice of the enclosing path  $C$ . Likewise, the topological charge of a phase saddle, maximum or minimum is always zero.

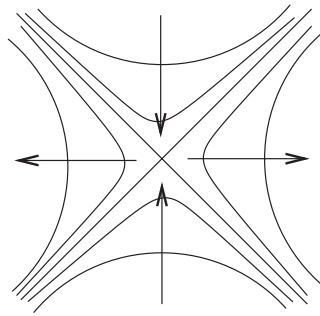
Another quantity of interest is the *topological index*  $t_E$ , which is defined as the topological charge of the phase singularities of the vector field  $\nabla \phi_E$ . It can be shown that for a positive or negative vortex  $t_E = +1$ , while for a phase saddle  $t_E = -1$ . The topological index of a phase maximum or minimum is  $t_E = +1$ .



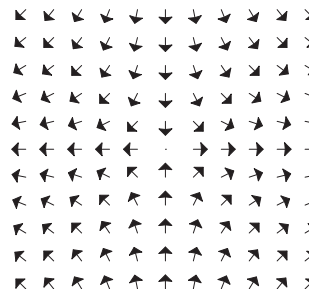
(a) positive phase vortex



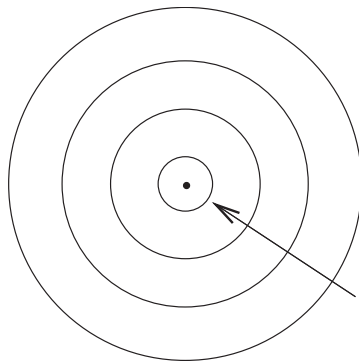
(b) left-handed power flow center



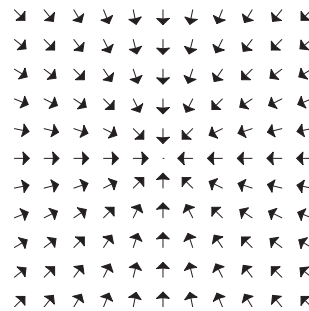
(c) phase saddle



(d) power flow saddle



(e) phase maximum



(f) power flow sink

Fig. 1. Illustrating the relation between phase singularities (a), stationary points of the phase (c,e), and the corresponding singularities of the power flow (b,d,f). The arrows in the left-hand column indicate the direction of increasing phase  $\phi_E$ .

A topological charge  $s_S$  and index  $t_S$  can also be associated with the phase  $\phi_S$  of the power flow. It follows directly from Eq. (5) that the topological *charge* of  $\mathbf{S}$  for a given feature is equal to the topological *index* of  $\hat{E}_y$ . The topological charge of a vortex of power flow is therefore  $s_S = +1$  regardless of whether it is a positive or negative vortex of  $\hat{E}_y$ . Similarly, the topological charge of a saddle point of power flow is  $s_S = -1$ , and the topological charge of a source or sink is  $s_S = +1$ . A topological index may be defined for the singularities of power flow, but is not necessary for our interests and will not be considered here.

Both topological charge and index are quantities which are conserved under smooth variations of the configuration parameters, and as such can only appear or disappear via creation and annihilation of multiple stationary and/or singular points. The most common process, which we will be primarily concerned with, involves the creation (annihilation) of a positive vortex ( $s_E = +1, t_E = +1$ ), a negative vortex ( $s_E = -1, t_E = +1$ ), and two phase saddles ( $s_E = 0, t_E = -1$  for each). This event may also be described in terms of the field of power flow as the creation (annihilation) of two centers of opposite direction ( $s_S = +1$  for each) with two saddle points ( $s_S = -1$ ). Other, more complex, events are possible, but are not typical.

### 3. Integral equation solution for the electromagnetic field near a slit

The configuration under consideration is illustrated in Fig. 2. An monochromatic electromagnetic wave is normally incident upon a metal plate of thickness  $d$  and permittivity  $\varepsilon_{\text{plate}}$  from the negative  $z$ -direction. A single slit of width  $w$ , infinitely long in the  $y$ -direction, is present in the plate. Because the system is invariant with respect to  $y$ -translations, we may treat the problem as two-dimensional, with relevant coordinates  $x$  and  $z$ .

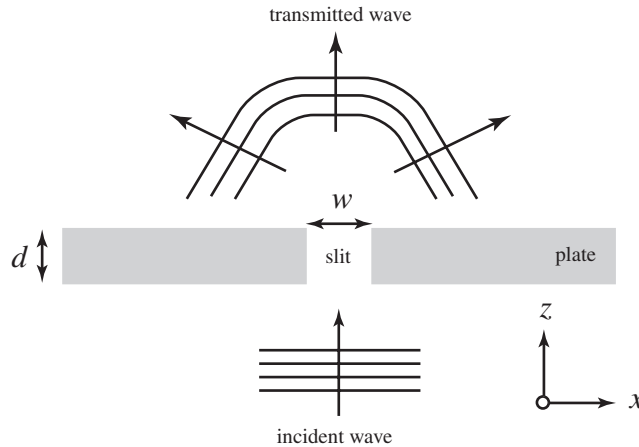


Fig. 2. Illustrating the notation relating to transmission through a slit.

The total electric field  $\hat{\mathbf{E}}$  may be written as the sum of two parts, namely the incident field,  $\hat{\mathbf{E}}^{\text{inc}}$ , and the scattered field,  $\hat{\mathbf{E}}^{\text{scatt}}$ . The incident field is here taken to be the field that would occur in the absence of the slit in the plate; it can readily be calculated analytically by use of the electromagnetic boundary conditions.

It can then be shown [9] that the  $i$ th component of the total field, denoted by  $\hat{E}_i(x, z)$ , satisfies an integral equation of the form

$$\hat{E}_i(x, z) = \hat{E}_i^{\text{inc}}(x, z) - i\omega\Delta\varepsilon \int_D \hat{G}_{ij}^E(x, z; x', z') \hat{E}_j(x', z') dx' dz', \quad (7)$$

where  $\Delta\varepsilon = \varepsilon_0 - \varepsilon_{\text{plate}}$  is the difference between the vacuum permittivity and the permittivity of the metal plate,  $\hat{G}_{ij}^E$  is the electric Green's tensor pertaining to the plate without the slit, and the integration is over the domain of the slit  $D$ . For points which lie within the slit, Eq. (7) is a Fredholm equation of the second kind for  $\hat{\mathbf{E}}$ , which can be solved numerically by the collocation method with piecewise-constant basis functions. The electric field outside the domain of the slit may then be calculated by substituting this solution back into Eq. (7). With the electric field determined everywhere, the magnetic field everywhere follows directly from Maxwell's equations. The Poynting vector may then be calculated using Eq. (1).

The definition of the transmission coefficient of the slit consists of two parts: the first is the integral of the normal component of the actual time-averaged Poynting vector  $\mathbf{S}$  over the slit, and the second is the difference of the normal components of the actual time-averaged Poynting vector and that of the Poynting vector in the absence of the slit,  $\mathbf{S}^{\text{inc}}$ , integrated over the dark side of the plate (not the region of the slit). The result is normalized by the normal component of  $\mathbf{S}^{(0)}$ , the Poynting vector of the field emitted by the source and impinging on the slit, i.e.

$$T \equiv \frac{\int_{\text{slit}} S_z \, d^2x + \int_{\text{plate}} (S_z - S_z^{\text{inc}}) \, d^2x}{\int_{\text{slit}} S_z^{(0)} \, d^2x}. \quad (8)$$

The subtraction in the second integral in the numerator corrects for the small part of the incident field which may flow through the plate itself.

With calculations of the power flow in the neighborhood of the slit and of the transmission coefficient, we are now able to demonstrate the relation between phase singularities and enhanced transmission (see also Ref. [10]).

#### 4. Phase singularities near sub-wavelength slits

An example of the field of power flow (i.e., the time-averaged Poynting vector) near a narrow slit in a thin plate of evaporated silver is shown in Fig. 3. In this example the incident field is taken to be TE polarized (i.e., with the  $\hat{\mathbf{E}}$  field parallel to the slit). It follows from the structure of  $\hat{G}_{ij}^E$  that the scattered field is then also TE polarized implying that the analysis of Section 2 applies. It can be seen from Fig. 3 that the field exhibits several phase singularities, namely vortices and saddles. In addition, the aperture is seen to have a funnel-like effect on the field, corresponding to a transmission coefficient  $T = 1.11$ . When the slit width is increased in a continuous manner, the four singularities below the slit (in the region indicated by the box) move together and finally annihilate each other. After the annihilation takes place, a smoother field of power flow results, corresponding to a greater transmission coefficient. This process is shown in Fig. 4. It can be seen that the transmission takes on a maximum value of  $T = 1.33$  when the slit width is  $w = 0.5\lambda$ .

Figure 5 shows the location of different kinds of phase singularities for the same configuration on a larger scale. In Fig. 6 the creation, movement, and subsequent annihilation of the phase singularities of the field of power flow are shown when the slit width is gradually increased. The slit width  $w$  and the corresponding power transmission coefficient  $T$  are also shown. Three groups of singularities obstruct the power flow directly in front of the slit; these groups each annihilate at  $w = 0.42\lambda$ ,  $w = 0.43\lambda$ , and  $w = 0.46\lambda$ . Only when they have disappeared does the transmission show anomalously high behavior.

The two movies presented here clearly show that anomalous light transmission through a sub-wavelength slit is accompanied by annihilation of singularities of the field of power flow in the immediate neighborhood of the slit. It is to be noted that, for

the choice of polarization that was analyzed, no surface plasmons are generated in the metal plate. Our study demonstrates that anomalous light transmission can even occur in their absence.

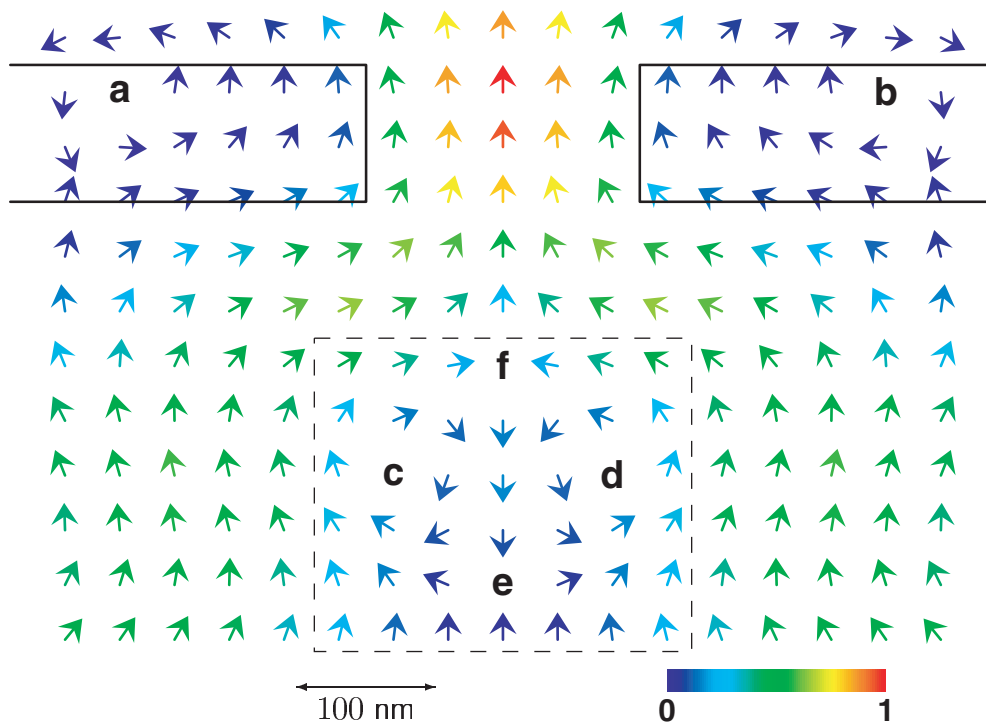


Fig. 3. Illustration of the power flow in the neighborhood of a 200 nm wide slit in a 100 nm thick plate of evaporated silver, with wavelength  $\lambda = 500$  nm and  $n = 0.05 + i2.87$  (the value of the refractive index was taken from [11]). Features (a) and (d) are left-handed centers, (b) and (c) are right-handed centers, and (e) and (f) are saddles. For this example the transmission coefficient  $T = 1.11$ . The color coding indicates the modulus of the (normalized) Poynting vector. The dashed box indicates the region illustrated in Movie 1.

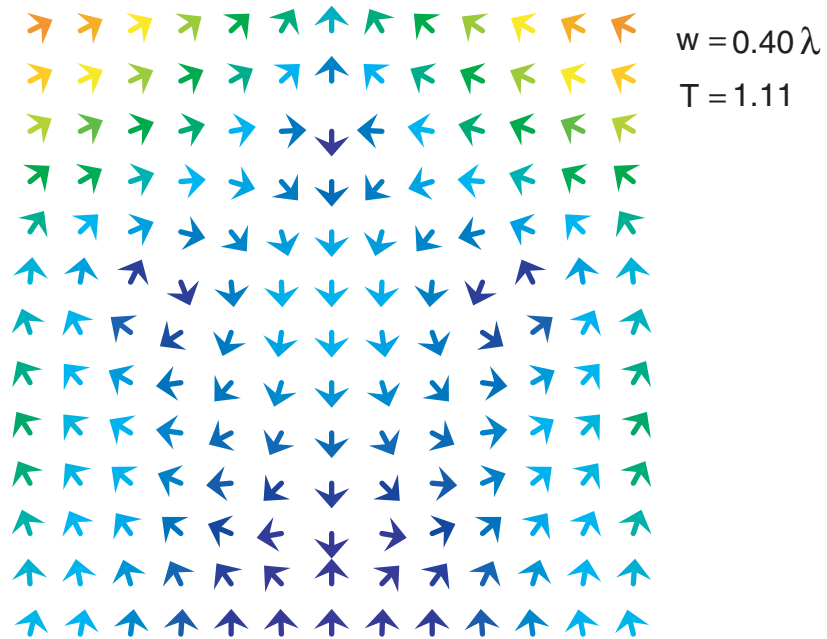


Fig. 4. (186 KB) The field of power flow as a function of the slit width  $w$  in the region indicated in Fig. 3. The four phase singularities move together as the slit width is increased, and finally annihilate, leaving a smoother field of power flow corresponding to a higher transmission coefficient  $T$ .

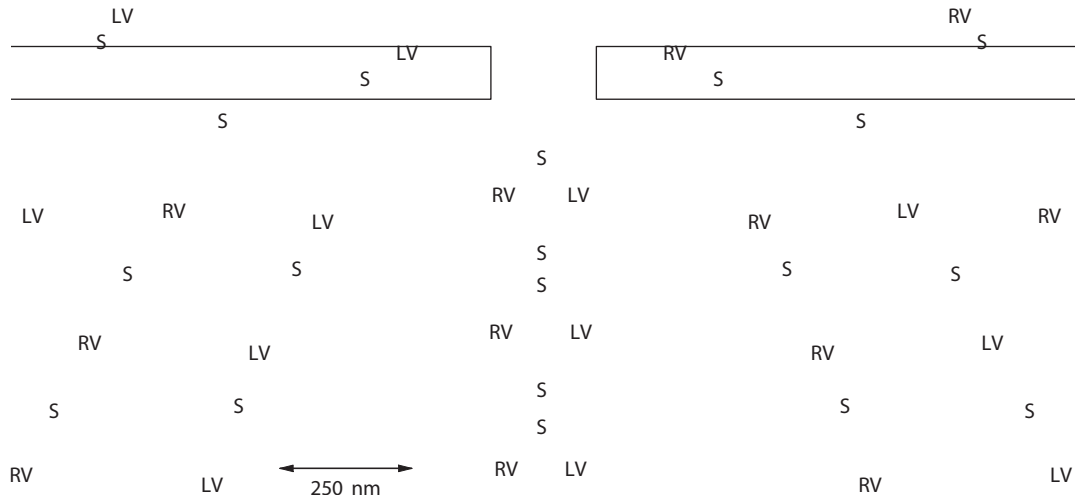


Fig. 5. Array of singularities in the field of power flow in the neighborhood of the slit. All parameters are as given in Fig. 3. Left-handed vortices (centers) and right-handed vortices (centers) are denoted by LV and RV, respectively, and saddles are denoted by S.

$$w = 0.01 \lambda$$
$$T = 0.01$$

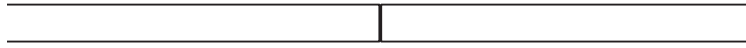


Fig. 6. (212 KB) Schematic of the position and type of singularities of power flow near a sub-wavelength slit. It is to be observed that multiple creation and annihilation events occur as the slit width is gradually increased. Left-handed vortices (centers) and right-handed vortices (centers) are denoted by LV and RV, respectively, and saddles are denoted by S. U denotes a vortex (center) very close to a saddle point which cannot be spatially resolved by the particular grid used for these calculations; it can be seen that eventually the singularities separate sufficiently to be distinguishable.

### Acknowledgements

This research was supported by the Dutch Technology Foundation (STW), and by the European Union within the framework of the Future and Emerging Technologies-SLAM program